Confocal Laser Scanning Microscopy (CLSM), a tool for counterfeit detection

M. Simard-Normandin and R. Rahman
MuAnalysis
Ottawa, Ontario, Canada
martine@muanalysis.com

ABSTRACT

This paper explains the CLSM technique and presents surface roughness measurement data from several groups of known authentic and suspect counterfeit parts. Surface roughness is an important characteristic of plastic encapsulated or metal lidded parts because counterfeit parts are often blacktopped or re-polished and remarked.

Key words: Counterfeit components, laser microscopy, confocal laser scanning microscopy, CLSM.

INTRODUCTION

This work is done in part for the SAE G19A committee. A series of test method documents are being prepared to complement the AS6171 standard [1]. One such document is SAE AS6171/17 Technique for Suspect/Counterfeit EEE Parts Detection by Laser Scanning Microscopy (LSM) and Confocal Laser Scanning Microscopy (CLSM) Test Methods [2]. The aim of the document is to provide guidance for those using these techniques for counterfeit detection. However, there is little data available for comparison in the literature on counterfeit detection using these techniques. This paper will focus on providing CLSM roughness data. Many devices, known authentic and suspect counterfeit parts, were measured.

CONFOCAL LASER SCANNING MICROSCOPY

Laser Scanning Microscopy (LSM) is a digital microscopy technique. A focused laser beam is raster scanned on a sample and the reflected light analyzed by a detector (Figure 1). The result is a matrix of light intensity at each collection point or pixel. When a pinhole is introduced at the focal point of the light path before the detector, the only light reaching the detector is from parts of the sample that are in "perfect" focus and the technique becomes confocal LSM or CLSM (Figure2). By collecting images at a series of focal planes, a 3D reconstruction of the surface is possible. Therefore, CLSM is a non-contacting profilometry technique.

LSM and CLSM are optical techniques. Therefore, the achieved spatial resolution depends on the wavelength of the laser used and is generally in the 1 micrometer range. Analysis is done in air. There is no need for vacuum, thus allowing easier analysis of large samples.

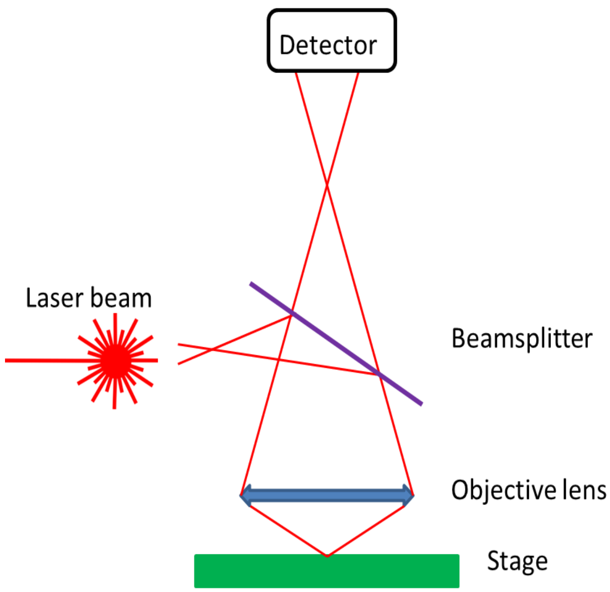

Figure 1. Typical LSM layout

On a polished, flat surface with sub-micrometer surface roughness (such as a microscope slide), the LSM and CLSM modes provide similar results because the entire surface will be in focus. If the sample has surface roughness on the order of micrometers or greater, then the CLSM technique will result in the detector receiving little light from regions (hills and valleys) which are not at the focal point of the pinhole.

CSLM can be used to compare surface roughness of devices, depth of laser markings, curvature and warping in the micrometer range. This can be particularly useful when known authentic parts are available for comparison purposes.

Counterfeit devices are often resurfaced and remarked. CLSM data allows quantitative measurements of the surface texture of devices, providing a basis for comparison to exemplars or to similar devices of known origin.

Presented at ISTFA 2018.

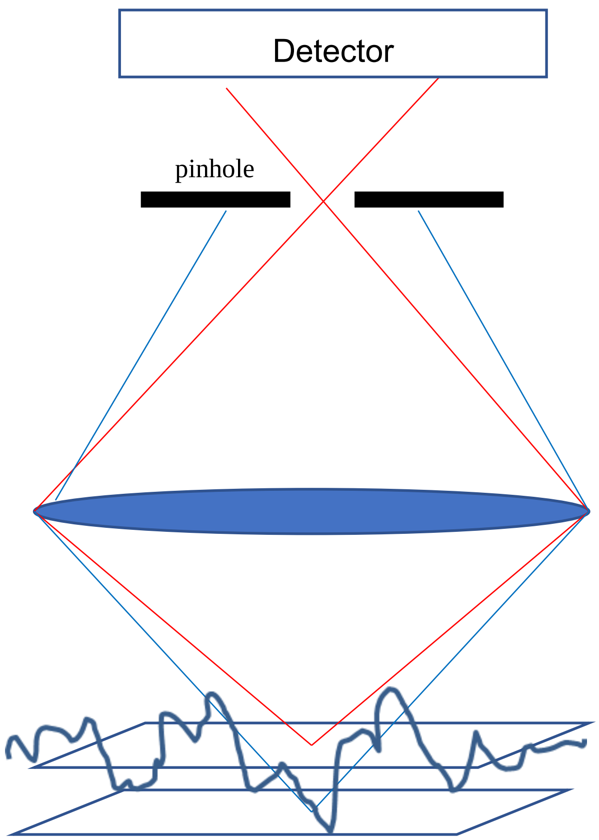

Figure 2. CLSM set-up with the pin-hole in place. Pixels not in the focal plane reflect less light and are blocked by the pin hole. The laser is omitted for clarity.

ROUGHNESS PARAMETERS

The texture of a random surface is expressed in terms of roughness parameters calculated from the height of the samples at a collection of points. The most common parameters are:

- zm = mean height of the surface = (z1+z2+…)/n

- Rq = root mean square roughness = sqrt{[$(z1\text{-}zm)^2$ + $(z2\text{-}zm)^2$+…]/n}

The root mean square (RMS) roughness, which is the average between the height deviations and the mean surface, taken over the evaluation area.

- Ra = arithmetic mean roughness =(|z1-zm| + |z2-zm|+…)/n

The arithmetic mean roughness (average roughness), which is the height as calculated over the entire measured length/area.

- Rt = zmax-zmin

Maximum roughness, which is the vertical distance between the highest point (Zmax) and the lowest point (Zmin) in the evaluation length/area.

Presented at ISTFA 2018.

- Rmax=max surface roughness= MAX(zmax1-zmin1 ,zmax2-zmin2 ,…,zmax5-zmin5)

Maximum Roughness Height within a sample length. This parameter is calculated during a single sample length measurement. The sample length is divided into 5 equal segments called cutoff traces. The vertical distance from the maximum peak to the lowest valley in each cutoff trace is calculated. The reported value is the maximum of the five Rmax (Ry) values.

- Rz= average surface roughness= (zmax1-zmin1 +zmax2-zmin2 +…+zmax5-zmin5)/5

The average maximum profile of the five greatest peak-to-valley separations in the evaluation area.

Where
- zi = height at position i (xi,yi)

THE DATASET

To obtain roughness parameters from known authentic parts and counterfeit parts, measurements have been taken from many parts. Some parts were received years ago directly from the manufacturers and are known to be authentic. Other parts are from unknown resellers. All the latter have features that make them suspect counterfeits. One difficulty encountered was to find older known authentic parts. Counterfeits parts are more likely to be found among obsolete or difficult to find parts.

Description	No. of parts	Status
ATI BGA	8	Authentic
Samsung BGA memory	10	Suspect counterfeit
Nortel PQFP	9	Authentic
Atmel 4 PQFP	4	Suspect counterfeit
Atmel 2 PQFP	8	Suspect counterfeit
Atmel 3 PQFP	8	Suspect counterfeit
OKI PLCC	9	Suspect counterfeit
NEC Gull Wing	5	Suspect counterfeit

Table 1. Parts used in this study

For each device these six roughness parameters (Zm, Rq, Ra, Rt, Rmax, Rz) were obtained at each corner and in the center. Front and back surfaces were measured in all, but in the BGA devices, where only the front was measured. The measurements were done using a Zeiss 310 laser scanning microscope in confocal mode. The illumination was from a 632nm He-Ne laser. Measurements were done using a 50x objective lens, giving a field of view of about 250x250µm. A scan rate of 2 seconds was used, and 50 image planes were acquired, 1µm apart. All measured values are in µm. Zm is given for completeness but carries little information since all devices are mostly flat and were measured under identical conditions.

RESULTS

The two BGAs: ATI and Samsung

There is a distinct difference in surface texture between the ATI parts, known to be authentic and the Samsung parts, almost certainly remarked (they have Sn-Pb balls, but the markings indicate lead-free).

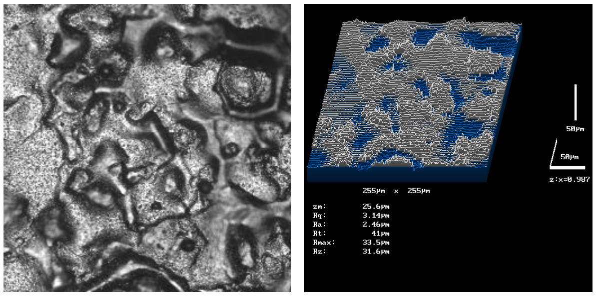

ATI front surface

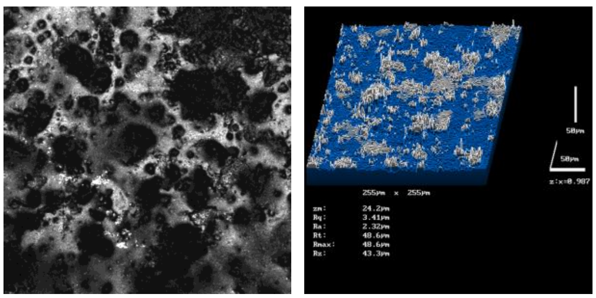

Samsung front surface

Figure 3. CLSM images and corresponding topography scans. Top: ATI part, bottom Samsung part. An artificial water level is added for clarity.

		Zm	Rq	Ra	Rt	Rmax	Rz
ATI	mean	25.99	3.45	2.75	37.82	36.10	31.69
ATI	st.dev	2.25	0.32	0.28	5.19	4.94	3.86
Samsung	mean	25.67	2.75	1.87	42.38	41.12	36.00
Samsung	st.dev	1.19	0.42	0.29	4.78	4.97	4.57

Table 2. Comparison of mean and standard deviations of the parameters. Rq and Ra are smaller in the Samsung part but Rt, Rmax and Rz are larger. All values are in µm.

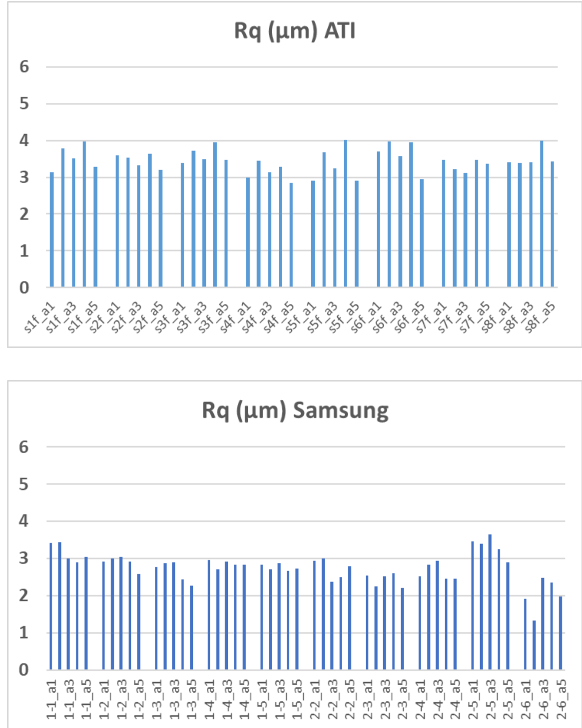

Figure 4. Comparison histograms of Rq measurements. Top: ATI, bottom: Samsung. Each group of five bars represents the measurements on one device at the four corners and the center. The center measurement is the fifth bar.

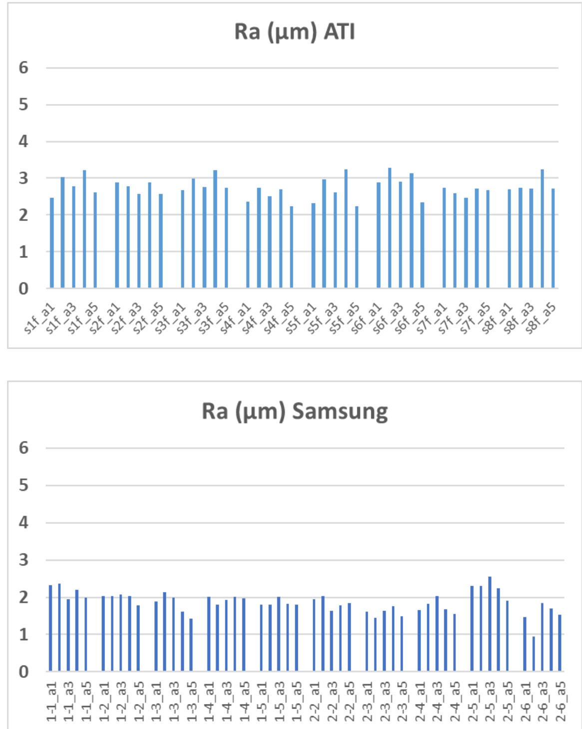

Figure 5. Comparison histograms of Ra measurements. Top: ATI, bottom: Samsung.

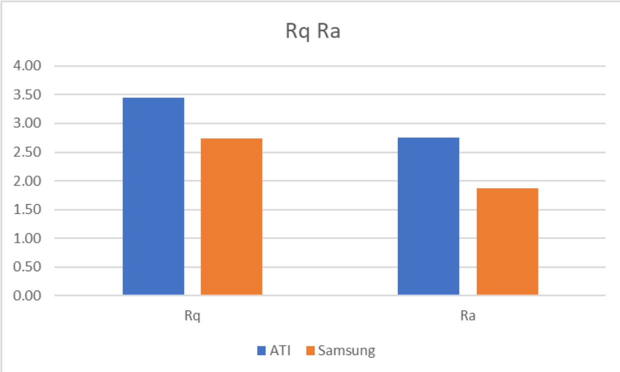

Figure 6. Histograms of the mean parameters Rq and Ra. Left: front measurements, Right: back measurements.

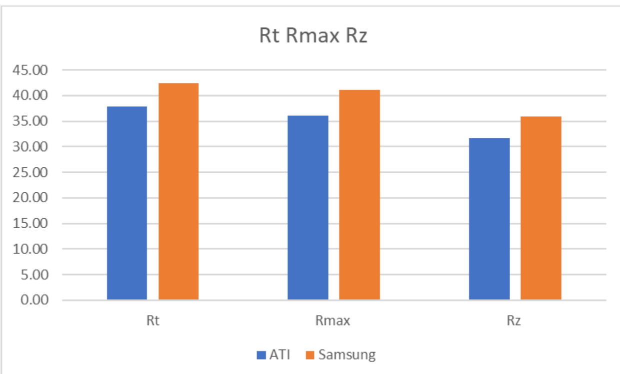

Figure 7. Histograms of the mean parameters Rt, Rmax and Rz. Left: front measurements, Right: back measurements.

The Samsung devices show scratches as evidence of grinding in some locations. The CLSM data provides quantitative data describing the texture of a ground plastic part.

Nortel and OKI

For injection molded parts, comparison of the front and back surfaces can yield significant information. The pins make it more difficult to grind and polish the back surface, which often leads counterfeiters to resurface only the front, resulting in measurable differences between the two surfaces. The OKI devices in this study are PLCC devices. The J pins make back resurfacing quite difficult.

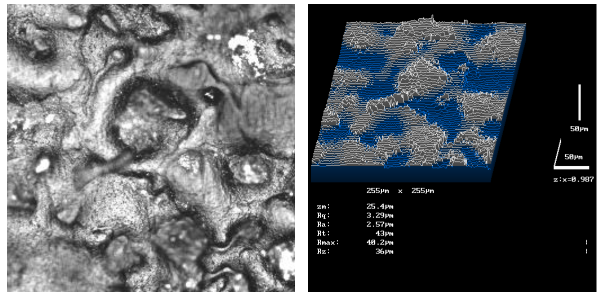

Nortel front surface

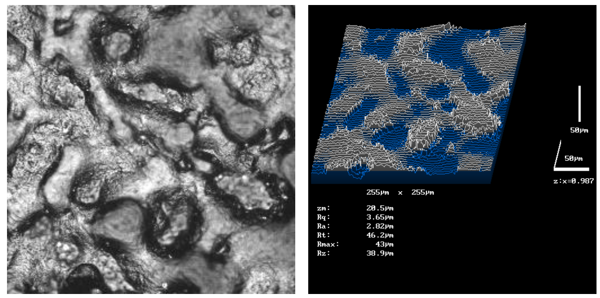

Nortel back surface

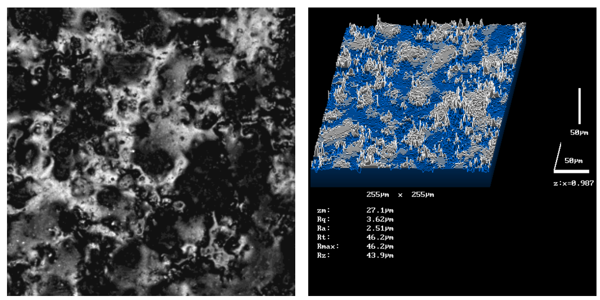

OKI front surface

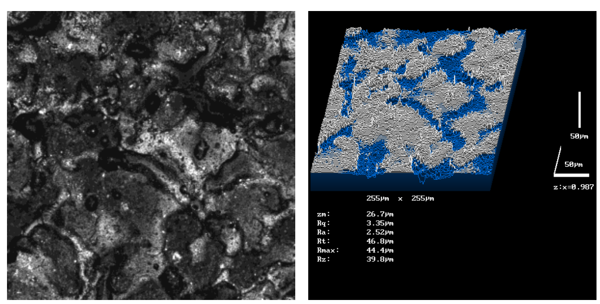

OKI back surface

Figure 8. CLSM images and topography scans. Top two: Nortel front and back, Bottom: OKI front and back. The OKI has a distinct difference in texture between the front and the back.

		Zm	Rq	Ra	Rt	Rmax	Rz
Nortel F	mean	23.15	2.96	2.31	39.68	38.09	31.43
Nortel F	st.dev	3.07	0.49	0.41	5.64	5.63	4.22
OKI F	mean	25.26	3.92	2.72	48.33	48.21	45.57
OKI F	st.dev	1.24	0.57	0.48	1.44	1.51	1.95
Nortel B	mean	23.56	3.58	2.85	42.98	41.54	35.22
Nortel B	st.dev	2.29	0.50	0.42	4.43	4.47	4.42
OKI B	mean	25.36	3.18	2.45	43.93	42.28	36.02
OKI B	st.dev	1.63	0.32	0.24	4.38	4.85	3.66

Table 3. Comparison of mean and standard deviations of the parameters. All values are in µm.

Rq and Ra are marginally smaller in the Nortel part front but Rt, Rmax and Rz are significantly larger in the OKI. There are very little differences between the parameters taken on the back of both devices. The OKI back parameters Rt, Rmax and Rz are not significantly different from the Nortel front parameters.

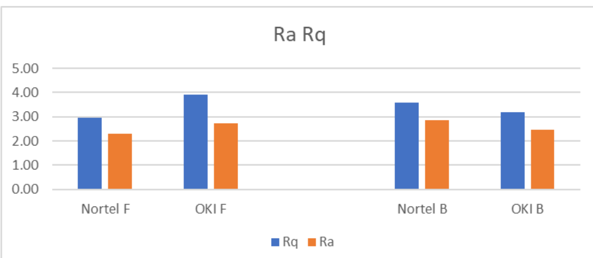

Figure 9. Histograms of the mean parameters Ra and Rq. Left: front measurements, Right: back measurements.

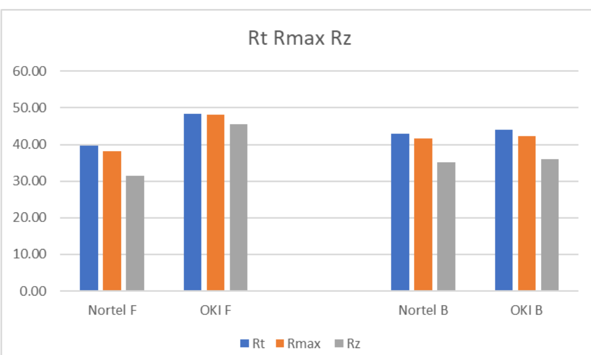

Figure 10. Histograms of the mean parameters Rt, Rmax and Rz. Left: front measurements, Right: back measurements.

The front of the OKI part shows evidence of grinding.

Three ATMEL codes compared to Nortel

Visually, the texture of the three codes of Atmel devices looks like that of the Nortel devices. There are also no big differences between the front and the back of the devices. However, it is suspected that they have been blacktopped, but it is very well done. There is no residue in markers, but scratches are seen there, which is consistent with parts that had been subjected to grinding. The Atmel 2 devices are known to be counterfeits based on die level evidence.

Presented at ISTFA 2018.

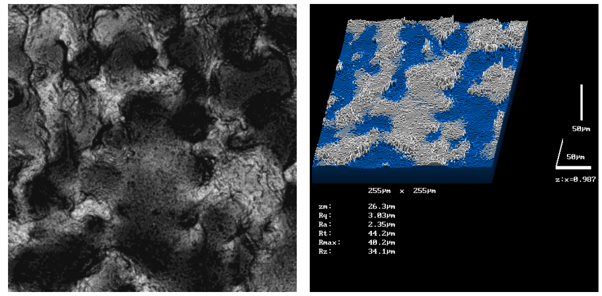

Atmel 2 front surface

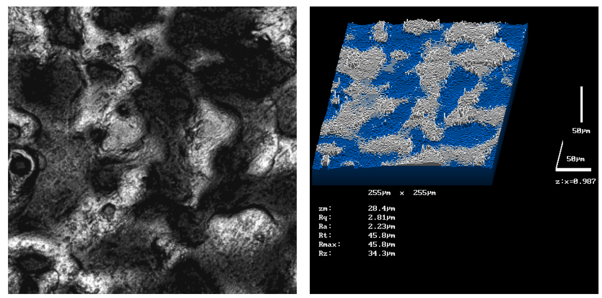

Atmel 2 back surface

Figure 11. Atmel 2 front and back

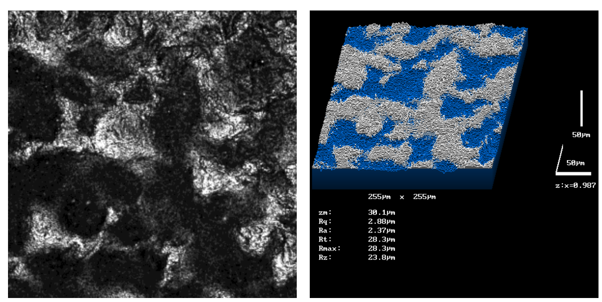

Atmel 3 front surface

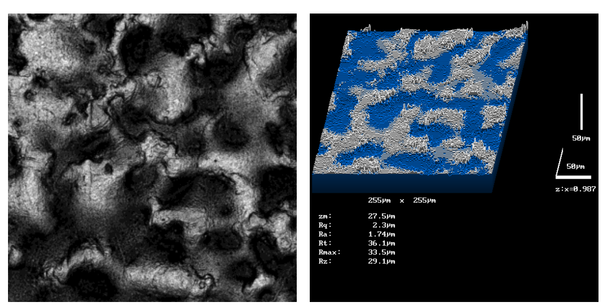

Atmel 3 back surface

Figure 12. Atmel 3 front and back

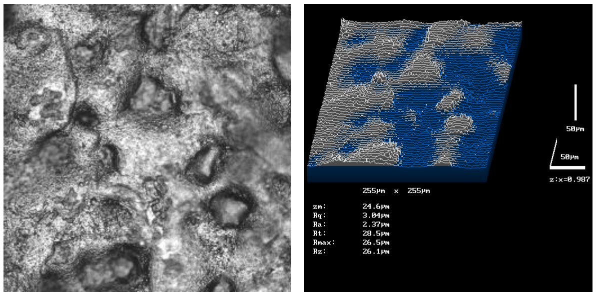

Atmel 4 front surface

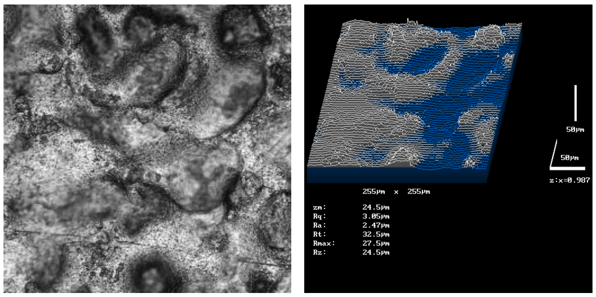

Atmel 4 back surface

Figure 13. Atmel 4 front and back

		Zm	Rq	Ra	Rt	Rmax	Rz
Nortel F	mean	23.15	2.96	2.31	39.68	38.09	31.43
Nortel F	st.dev	3.07	0.49	0.41	5.64	5.63	4.22
Atmel 2 F	mean	27.08	2.97	2.37	35.64	34.19	28.82
Atmel 2 F	st.dev	1.47	0.34	0.31	4.76	4.49	3.30
Atmel 3 F	mean	26.75	3.14	2.49	38.51	37.11	31.98
Atmel 3 F	st.dev	1.46	0.32	0.25	6.37	6.26	4.76
Atmel 4 F	mean	25.01	3.19	2.45	38.34	36.99	30.61
Atmel 4 F	st.dev	1.78	0.86	0.60	6.25	5.95	4.50
Nortel B	mean	23.56	3.58	2.85	42.98	41.54	35.22
Nortel B	st.dev	2.29	0.50	0.42	4.43	4.47	4.42
Atmel 2 B	mean	26.50	2.75	2.18	35.57	34.48	27.96
Atmel 2 B	st.dev	1.62	0.29	0.21	6.55	6.24	4.41
Atmel 3 B	mean	26.17	2.33	1.82	33.82	31.56	27.02
Atmel 3 B	st.dev	0.82	0.39	0.31	6.79	7.61	5.12
Atmel 4 B	mean	25.02	2.85	2.22	37.02	35.18	29.98
Atmel 4 B	st.dev	1.56	0.52	0.40	6.50	6.06	4.81

Table 4. Comparison of mean and standard deviations of the parameters. F: front, B: back. All values are in µm.

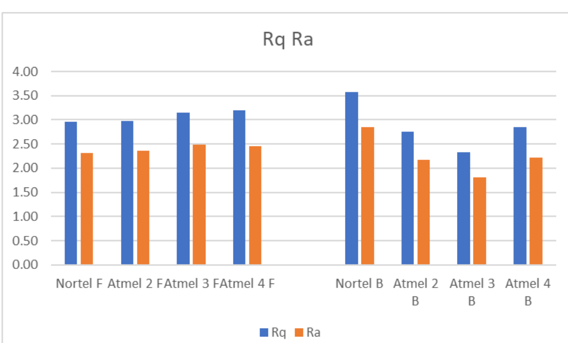

Figure 14. Histograms of the mean parameters Ra and Rq. Left: front measurements, Right: back measurements.

Presented at ISTFA 2018.

It is difficult to come to a definite conclusion based on these averages. The distributions have more information.

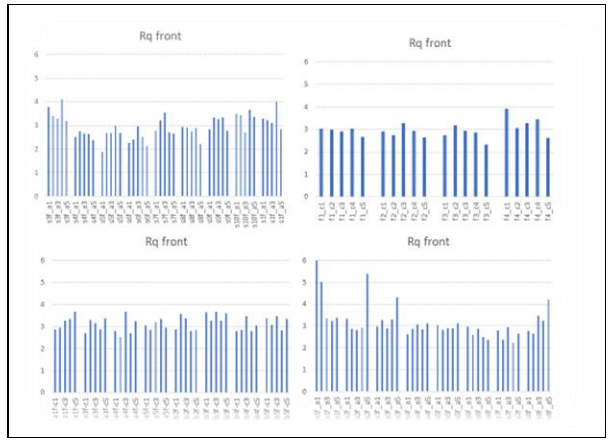

Figure 15. Front surface Rq values comparing Nortel (upper left corner) to all three Atmel devices. Atmel2 upper right, Atmel 3 lower left, Atmel 4 lower right. The Y scale is 0-6µm for all Ra and Rq graphs.

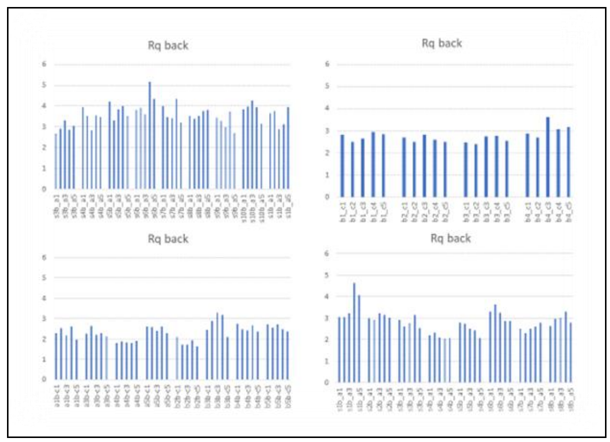

Figure 16. Back surface Rq values comparing Nortel (upper left corner) to all three Atmel devices.

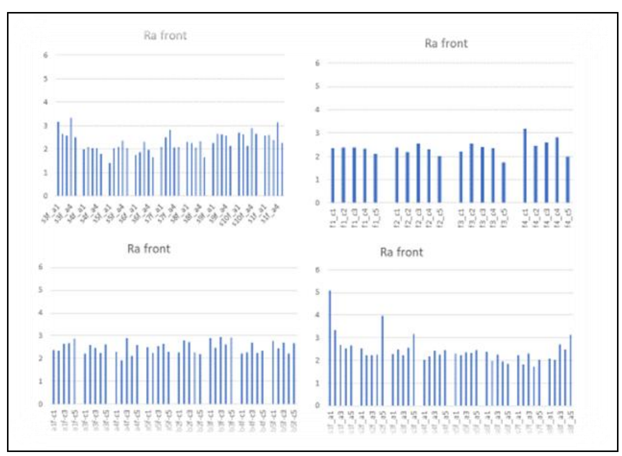

Figure 17. Front surface Ra values comparing Nortel (upper left corner) to all three Atmel devices.

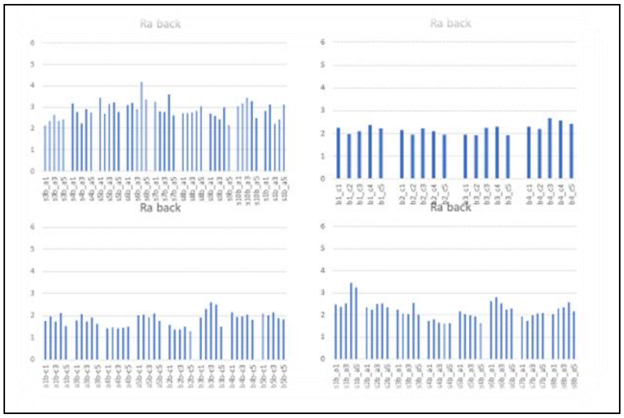

Figure 18**.** Back surface Ra values comparing Nortel (upper left corner) to all three Atmel devices.

The distribution of Ra and Rq values from the front side are very similar for all 4 parts. The back-side values of the Atmels are different from the Nortel. The difference is more substantial in Atmel 3.

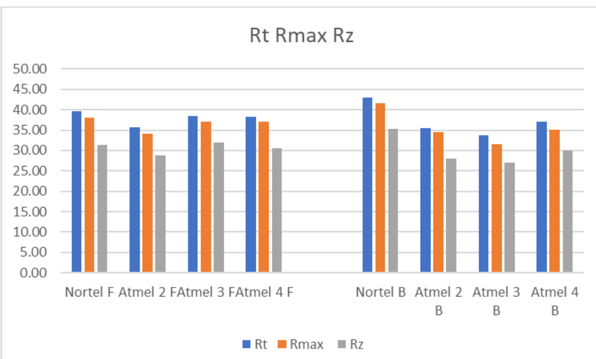

Figure 19. Histograms of the mean parameters Rt, Rmax and Rz. Left: front measurements, Right: back measurements.

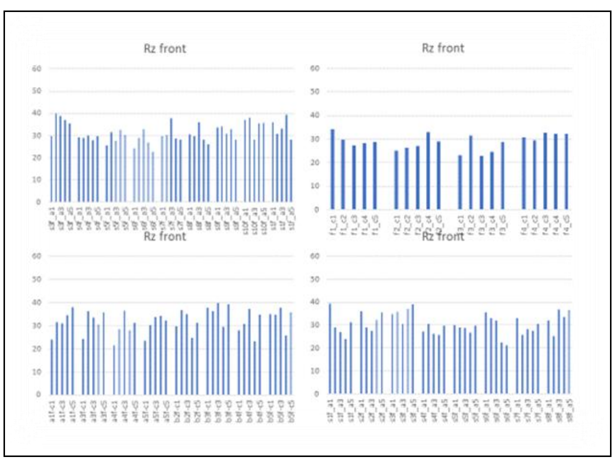

Figure 20. Front surface Rz values comparing Nortel (upper left corner) to all three Atmel devices. No significant differences of population are observed. The Y scale is 0-60 µm for all Rz graphs.

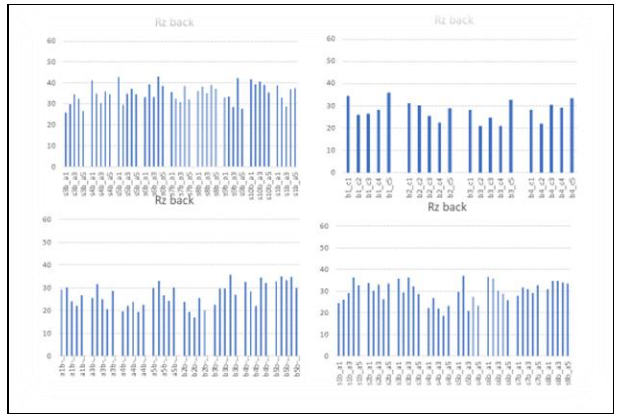

Figure 21. Back surface Rz values comparing Nortel (upper left corner) to all three Atmel devices.

The Atmel devices look like the Nortel parts on the front, but the back is different. The distribution of values from the back side shows differences indicating a different type of population between the front and back surfaces in the Atmel parts. This supports the suspicion that the Atmel parts have been altered.

Nortel and NEC

The NEC device is an opto-isolator. There is a cavity within the device to allow the light emitted by the LED to reach the photodetector. Although it is a plastic encapsulated device, it is not assembled like a PQFP, which is the only known authentic device in this study.

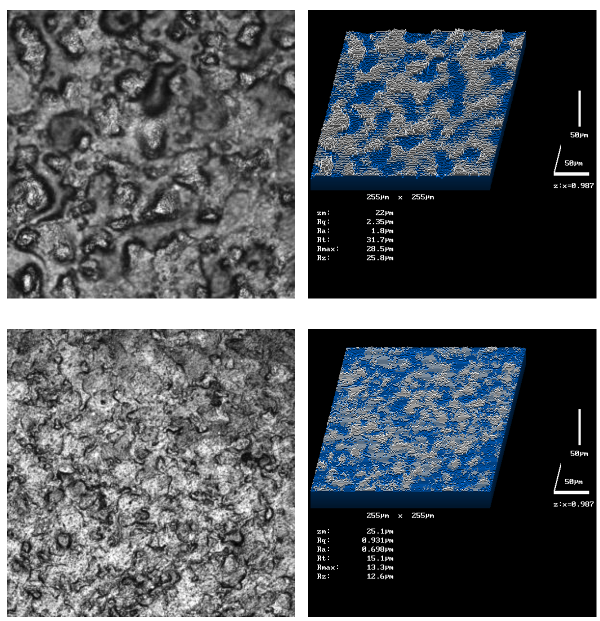

Figure 22. NEC front and back.

		Zm	Rq	Ra	Rt	Rmax	Rz
Nortel F	mean	23.15	2.96	2.31	39.68	38.09	31.43
Nortel F	st.dev	3.07	0.49	0.41	5.64	5.63	4.22
NEC F	mean	25.31	1.95	1.51	27.72	26.95	22.13
NEC F	st.dev	1.89	0.46	0.35	8.04	8.16	5.24
Nortel B	mean	23.56	3.58	2.85	42.98	41.54	35.22
Nortel B	st.dev	2.29	0.50	0.42	4.43	4.47	4.42
NEC B	mean	25.75	1.38	1.05	23.90	22.97	17.61
NEC B	st.dev	0.94	0.37	0.30	7.20	7.18	4.11

Table 5. Comparison of mean and standard deviations of the parameters.

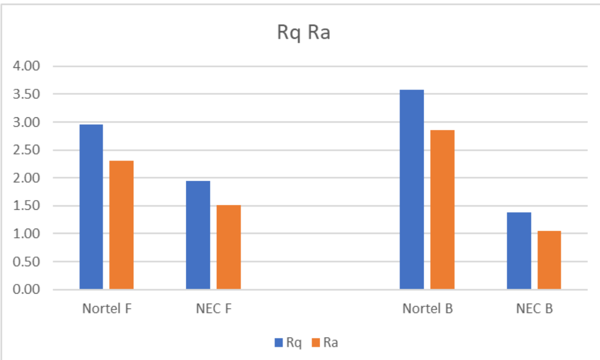

Figure 23. Histograms of the mean parameters Ra and Rq.

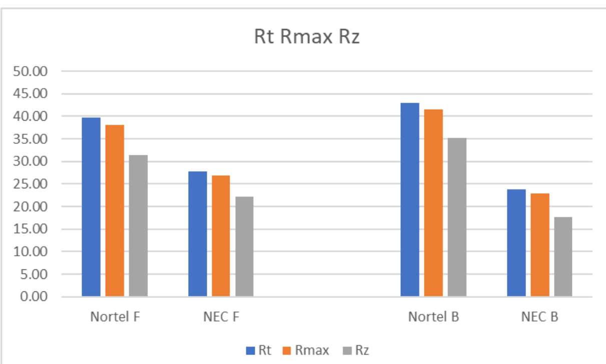

Figure 24. Histograms of the mean parameters Rt, Rmax and Rz.

Without an exemplar device and with only five devices available for analysis, no definite conclusion can be reached about this device. There is no evidence of grinding, but it could be blacktopped.

CONCLUSION

Identification of a part as a counterfeit requires input from several techniques. It is easier when exemplars of the same vintage are available, but this is often not the case.

CLSM roughness profiles provide quantitative data to compare parts that *do not look the same*. Even in the absence of exemplars CLSM reveals subtle differences that add to the ensemble of observations used to evaluate the authenticity of a part.

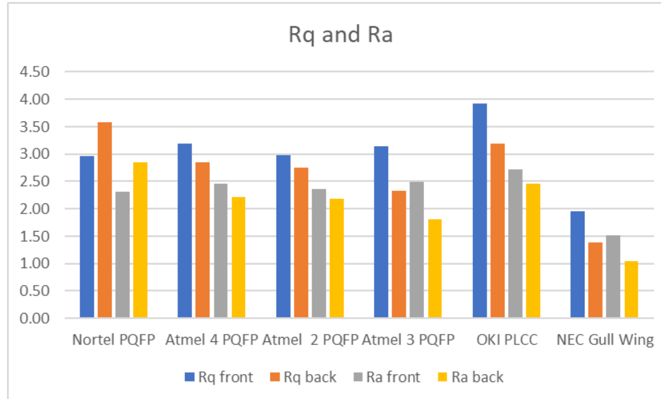

Figure 25. Average Rq and Ra parameters for the pin devices. All groups, except the authentic Nortel, have a similar distribution of parameters.

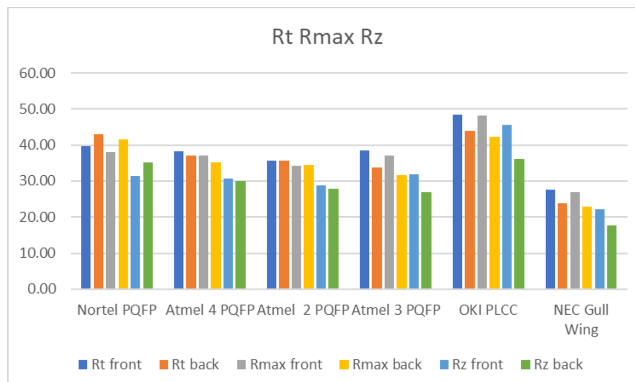

Figure 26**.** Average Rt, Rmax and Rz parameters for the pin devices. All groups, except the authentic Nortel, have a similar distribution of parameters.

Five hundred and twenty (520) CLSM profiles were taken on a collection of eight (8) codes of plastic encapsulated devices to provide examples of roughness parameters from authentic and suspect counterfeit parts. It is recognized that this is still a very small dataset. There is no shortage of suspect counterfeit parts to analyze but finding known authentic older parts is difficult. As more data becomes available, categories of surface parameters will emerge, making counterfeit detection more straightforward.

REFERENCES

1. SAE AS6171 Test Methods Standard; General Requirements, Suspect/Counterfeit, Electrical, Electronic, and Electromechanical Parts. Issued 2016-10-30. https://www.sae.org/standards/content/as6171/

2. SAE AS6171/17 Technique for Suspect/Counterfeit EEE Parts Detection by Laser Scanning Microscopy (LSM) and Confocal Laser Scanning Microscopy (CLSM) Test Methods In draft

Presented at ISTFA 2018.